

# Bio-electrochemical COD removal for energy-efficient, maximum and robust nitrogen recovery from urine through membrane aerated nitrification

Jolien De Paepe<sup>a,b,c</sup>, Kim De Paepe<sup>a</sup>, Francesc Gòdia<sup>b</sup>, Korneel Rabaey<sup>a,c,\*</sup>, Siegfried E. Vlaeminck<sup>c,d</sup>, Peter Clauwaert<sup>a,c</sup>

<sup>a</sup> Center for Microbial Ecology and Technology (CMET), Department of Biotechnology, Faculty of Bioscience Engineering, Ghent University, Coupure Links 653, 9000 Gent, Belgium

<sup>b</sup> Departament d'Enginyeria Química, Biològica i Ambiental, Escola d'Enginyeria, Universitat Autònoma de Barcelona, Bellaterra 08193 Barcelona, Spain

<sup>c</sup> Center for Advanced Process Technology and Urban Resource Efficiency (CAPTURE), Belgium

<sup>d</sup> Research Group of Sustainable Energy, Air and Water Technology, Department of Bioscience Engineering, University of Antwerp, Groenenborgerlaan 171, 2020 Antwerpen, Belgium

## ARTICLE INFO

### Article history:

Received 12 May 2020

Revised 17 July 2020

Accepted 23 July 2020

Available online 23 July 2020

### Keywords:

Resource recovery

Regenerative life support system

Nitrogen recovery

Yellow water

Source separation

Membrane biofilm reactor

## ABSTRACT

Resource recovery from source-separated urine can shorten nutrient cycles on Earth and is essential in regenerative life support systems for deep-space exploration. In this study, a robust two-stage, energy-efficient, gravity-independent urine treatment system was developed to transform fresh real human urine into a stable nutrient solution. In the first stage, up to 85% of the COD was removed in a microbial electrolysis cell (MEC), converting part of the energy in organic compounds (27–46%) into hydrogen gas and enabling full nitrogen recovery by preventing nitrogen losses through denitrification in the second stage. Besides COD removal, all urea was hydrolysed in the MEC, resulting in a stream rich in ammoniacal nitrogen and alkalinity, and low in COD. This stream was fed into a membrane-aerated biofilm reactor (MABR) in order to convert the volatile and toxic ammoniacal nitrogen to non-volatile nitrate by nitrification. Bio-electrochemical pre-treatment allowed to recover all nitrogen as nitrate in the MABR at a bulk-phase dissolved oxygen level below 0.1 mg O<sub>2</sub> L<sup>-1</sup>. In contrast, feeding the MABR directly with raw urine (omitting the first stage), at the same nitrogen loading rate, resulted in nitrogen loss (18%) due to denitrification. The MEC and MABR were characterised by very distinct and diverse microbial communities. While (strictly) anaerobic genera, such as *Geobacter* (electroactive bacteria), *Thiopsedomonas*, a *Lentimicrobiaceae* member, *Alcaligenes* and *Proteiniphilum* prevailed in the MEC, the MABR was dominated by aerobic genera, including *Nitrosomonas* (a known ammonium oxidiser), *Moheibacter* and *Gordonia*. The two-stage approach yielded a stable nitrate-rich, COD-low nutrient solution, suitable for plant and microalgae cultivation.

© 2020 Elsevier Ltd. All rights reserved.

## 1. Introduction

In recent years, source-separated urine has gained great interest as an alternative nutrient resource, reducing the need to mine (e.g., phosphorus and potassium) or to chemically synthesize nutrients consuming fossil fuels (e.g., natural gas for ammonia), while at the same time facilitating wastewater management and reducing environmental pollution (Maurer et al., 2006; Randall and Naidoo 2018). Urine is also an essential resource in regenerative life support systems for long-duration human Space missions, as

it presents the major flux of nitrogen in a regenerative life support system and contains additional macro- (i.e., phosphorus and potassium) and micro-nutrients (Clauwaert et al., 2017).

Without stabilization of urine, urea, the main nitrogen compound in urine, quickly hydrolyses into ammonia, ammonium and (bi)carbonate, causing nutrient losses, scaling and clogging by uncontrolled precipitation, ammonia volatilisation into the environment/Space cabin and odor nuisance (Udert et al., 2003b). Urine also contains organics (~10 g COD L<sup>-1</sup> (Udert et al., 2006) of which about 90% is biodegradable), fueling bacterial growth. Nitrification has been reported as a suitable method to stabilize urine, while preserving the nutrient content, and plays a pivotal role in the Micro-Ecological Life Support System Alternative (MELiSSA),

\* Corresponding author.

E-mail address: [korneel.rabaey@ugent.be](mailto:korneel.rabaey@ugent.be) (K. Rabaey).

the regenerative life support system program from the European Space Agency (ESA) (Coppens et al., 2016; De Paepe et al. 2018; Gòdia et al., 2002; Udert et al., 2003a; Udert and Wachter 2012). First, ammonium oxidizing bacteria (AOB) oxidize TAN (total ammonia nitrogen, i.e., sum of ammonia-N and ammonium-N) into nitrite (nitritation), which is subsequently oxidized into non-volatile and nontoxic nitrate (nitrification) by nitrite oxidizing bacteria (NOB). Simultaneously, biodegradable organics are oxidized to CO<sub>2</sub> by heterotrophic bacteria, decreasing the biofouling potential of urine.

Different reactor systems have been used for partial or full urine nitrification: continuous stirred tank reactors (Oosterhuis and van Loosdrecht, 2009, Udert et al., 2003), sequencing batch reactors (Chen et al., 2017, (Jiang et al., 2011, Mackey et al., 2010, Sun et al., 2012, Udert et al., 2003), moving bed biofilm reactors (De Paepe et al. 2018; Udert et al., 2003) and membrane bioreactors (Coppens et al., 2016; Fumasoli et al., 2016). In this study, urine nitrification was performed in a membrane-aerated biofilm reactor (MABR), given its high oxygen utilization efficiency, compact design and compatibility with the reduced gravity conditions in Space (Côté et al., 1988; Jackson et al., 2009; Martin and Nerenberg 2012; Nerenberg 2016). In an MABR, oxygen is transferred by diffusion through gas permeable membranes to the biofilm attached to the membrane outer surface. About 30–45 g O<sub>2</sub> L<sup>-1</sup> urine are required to oxidize all TAN and COD (chemical oxygen demand) in urine (assuming 6–9 g of N and COD L<sup>-1</sup>, and 4.33 g O<sub>2</sub> g<sup>-1</sup> N and 0.8 g O<sub>2</sub> g<sup>-1</sup> COD). MABR systems have been validated for nitrification, and for the removal of organics and/or nitrogen from numerous types of waste streams, including waste streams relevant for Space such as mixtures of urine, humidity condensate and surfactants (Chen et al., 2008; Christenson et al., 2018; Gong et al., 2007; Jackson et al., 2009; Pellicer-Nàcher et al., 2010). Due to their counter-diffusional biofilm, MABR systems are often used for simultaneous nitrification-denitrification (Casey et al., 1999). Over time, the biofilm thickness increases, and due to the oxygen consumption by nitrifiers and aerobic heterotrophs, residing deep in the biofilm close to the membrane surface, the outer layers of the biofilm (at the biofilm-liquid interface) become anoxic. In these layers, heterotrophic denitrifiers can convert the nitrate into nitrogen gas using COD as an electron donor. Nitrogen removal via nitrification-denitrification in an MABR has been investigated for water recycling from a Space-based waste stream, consisting of urine (10%), grey water and humidity condensate (Christenson et al., 2018; Jackson et al., 2009; Meyer et al., 2015). Thus far, only one study reported the use of an MABR for nitrogen recovery from urine. Udert and Wachter (2012) obtained partial nitrification and COD removal in an MABR operated on stored urine. Despite additional oxygen supply via bubble aeration to prevent anoxic zones, up to 24% of the nitrogen was lost by denitrification and nitrite accumulation occurred because of oxygen limitation (Udert and Wachter 2012).

Hence, avoiding the presence of anoxic zones in combination with bioavailable organics is critical in preventing a loss of nitrogen through denitrification. Therefore, a microbial electrolysis cell (MEC) was used in this study in order to remove the rapidly biodegradable COD prior to membrane-aerated nitrification. In the MEC, electrochemically active bacteria oxidize COD and use the anode as an electron acceptor (Logan et al., 2006). This way, chemical energy is converted into electrical energy, generating hydrogen gas at the cathode by applying a small potential with an external power supply (Logan et al., 2006). In recent years, a large number of studies on bio-electrochemical treatment (MEC and MFC) of (synthetic) urine were published. Since the main focus of most of these studies is energy recovery (Ieropoulos et al., 2012; Ieropoulos et al., 2016; Merino-Jimenez et al., 2017; Salar-García et al., 2017) or TAN recovery (Gao et al., 2018; Kuntke et al.,

2014; Kuntke et al., 2012; Kuntke et al., 2016; Ledezma et al., 2017), low COD removal efficiencies (<50%) are generally reported (Supplementary information (SI), Section J).

In this study, the goal was to achieve maximum nitrogen recovery at minimum energy expenditure. The aim for the MEC was therefore to achieve high COD removal efficiencies in order to prevent denitrification in the MABR. Two MEC configurations were evaluated in terms of COD removal, current production and nitrogen recovery, at a range of hydraulic residence times (HRT) and COD loadings. The MEC effluent was fed into a hollow fiber MABR for full nitrification (i.e., with base addition to convert all TAN into nitrate). Full nitrification was preferred over partial nitrification because of the higher process stability (optimal pH and no TAN accumulation) and safety (ammonium nitrate is thermally unstable which limits further concentration and it can be misused as an explosive) (Udert and Wachter 2012). The load of the MABR was gradually increased to evaluate the reactor performance at a low bulk dissolved oxygen (DO) concentration. Subsequently, raw urine was fed into the MABR to study the effect of the pre-treatment with the MEC. The microbial communities in both reactors were analysed using amplicon 16S rRNA gene Illumina sequencing.

## 2. Materials and methods

### 2.1. Experimental setup

#### 2.1.1. MEC1

MEC1 (Fig. 1A) was constructed of two Perspex® plates and frames with an internal volume of 200 mL (dimension of 20 × 5 × 2 cm<sup>3</sup>) separated by an ion exchange membrane (100 cm<sup>2</sup>, Ultrex CMI-7000 s or AMI-7001, Membranes International Inc., USA). The anodic compartment was filled with 200 g of graphite granules (Le Carbone, Belgium). Prior to use, the granules were washed with NaOH and HCl, rinsed with demineralised water and dried at 105 °C. A graphite felt (Alfa Aesar, Germany) and a stainless steel frame were used for electrical connection to a potentiostat (VSP, Biologic, France), which controlled the anode potential at -250 or -350 mV versus an Ag/AgCl reference electrode (ALS, Japan). The cathode consisted of a stainless steel wire mesh (564 µm mesh width, 20 × 5 cm<sup>2</sup>, Solana, Belgium). A peristaltic pump was used to recirculate the anolyte and catholyte through the recirculation vessels (glass bottles) and the anodic or cathodic compartment of the MEC. Urine was fed into the anode recirculation vessel with a peristaltic pump and a timer. The catholyte consisted of a phosphate buffer solution and was operated in a closed loop (i.e., without influent and effluent). The total volume of anolyte and catholyte were 740 or 490 mL and 1 L, respectively (Table 1).

#### 2.1.2. MEC2

MEC2 (Fig. 1B) was similar to MEC1 but the anode consisted of a graphite felt (100 cm<sup>2</sup>) (without granules) and a stainless steel wire mesh to collect the current. The two compartments were separated by a cation exchange membrane (CEM, Ultrex CMI-7000 s, Membranes International Inc., NJ, USA). The effluent of the anode recirculation vessel was directed into the cathode recirculation vessel. The total volume of anolyte and catholyte were 615 mL and 430 mL, respectively.

#### 2.1.3. MABR

The MABR was composed of three hollow fiber (HF) modules (SI Figure S1), consisting of 180 flow-through dense (non-porous) silicone rubber hollow fibers with a length of 25 cm, an inner diameter of 0.3 mm and an outer diameter of 0.5 mm (Nagasep M100, Nagayanagi Co., Japan). Each module was made from a plastic housing and had a total membrane surface area of 0.06 m<sup>2</sup> and

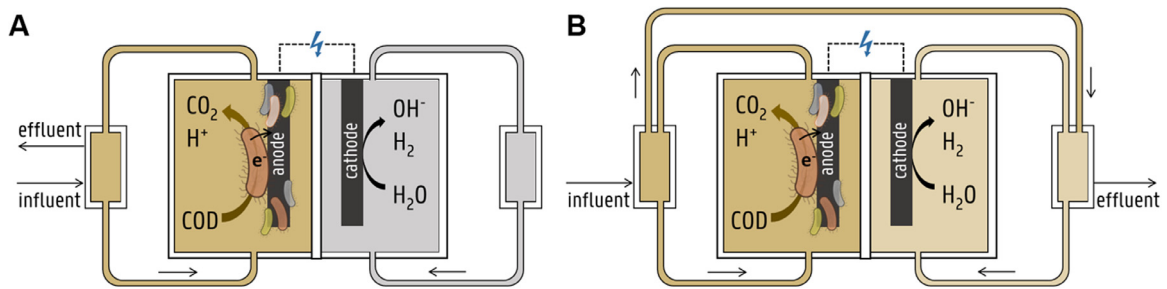


Fig. 1. Schematic overview of the microbial electrolysis cells MEC1 (A) and MEC2 (B).

Table 1

Overview of the different operational phases of MEC1 and MEC2. For MEC2, the HRT in the anodic compartment and total HRT (in anodic and cathodic compartment, value between brackets) are displayed. The average influent and effluent composition is reported in SI, Section B.

Phase	MEC	IEM	Anolyte volume [mL]	Anode potential [mV]	Influent flow rate [mL d <sup>-1</sup> ]	HRT [d]	Duration [d]	number of HRT
MEC1-CEM	1	CEM	740	-350	111	6.6	21	3.2
MEC1-AEM1	1	AEM	740	-350	110	6.7	27	4.0
MEC1-AEM2	1	AEM	490	-250	120	4.1	53	13.0
MEC1-AEM3	1	AEM	490	-250	133	3.7	20	5.4
MEC2-CEM1	2	CEM	615	-250	144	4.3 (7.3)	52	12.2 (7.2)
MEC2-CEM2	2	CEM	615	-250	241	2.5 (4.3)	25	9.8 (5.8)
MEC2-CEM3	2	CEM	615	-250	112	5.5 (9.4)	75	13.7 (8.0)

liquid volume of 90 mL. The liquid volume in the modules was hence 270 mL. The liquid was recirculated between the modules and two recirculation vessels (100 mL glass bottles) with a peristaltic pump at a flow rate of 11 L h<sup>-1</sup> (17 reactor volumes per hour). Including vessels, tubing and modules, the reactor had a total liquid volume of 650 mL. Humidified air was supplied through the lumen of the fibers in opposite direction of the liquid flow with aquarium pumps (air pump 400, EHEIM, Germany) at a flow rate of 0.65–0.75 L min<sup>-1</sup>. The bulk liquid DO concentration was monitored with a luminescent DO probe (LDO10103, Hach, Belgium) and a HQ40d meter (Hach, Belgium) and logged every five minutes. The pH was controlled at 6.85 by dosing 0.25 M NaOH with a Consort R3610 controller (Consort, Belgium) to obtain full nitrification. A pH setpoint of 6.85 was chosen to minimize the NaOH consumption and to reduce the risk for free ammonia (FA) inhibition in case of TAN accumulation. Influent was dosed with a peristaltic pump and a timer. After 168 days, one module was removed and sacrificed for sequencing, after which the MABR was operated with two modules (total liquid volume of 500 mL).

## 2.2. Reactor operation

### 2.2.1. Urine collection and alkalisation

Fresh urine from healthy male donors, not taking medication, was collected using a nonwater urinal with approval from the Ethical Committee of Ghent University Hospital (registration number B670201731862). Immediately after collection, batches of 2–4 L were prepared. The urine was diluted with demineralised water (33.3vol% urine; 66.6vol% water), simulating the diluting effect of flush water in urine diverting toilets (Wohlsager et al., 2010), and the pH was increased to above 11 with 2 M NaOH to prevent urea hydrolysis during storage (max. 2–3 weeks) at 4 °C prior to feeding into the MEC. The alkalisation step was included to avoid ammonia volatilisation (which can pose a hazard in Space), scaling and clogging due to uncontrolled precipitation, nutrient losses and malodour during storage. The pH increase also triggered controlled precipitation of calcium and magnesium salts, thereby minimizing the risk for scaling in the following treatment steps.

### 2.2.2. MEC operation

The anodic compartment of MEC1 was inoculated with effluent originating from an active MEC (fed with fermenter super-

natant) and operated in fed-batch mode on modified M9 medium (Guo et al., 2013) to establish an electroactive biofilm on the graphite granules. Subsequently, urine was fed into the anode recirculation vessel at 111 mL d<sup>-1</sup>. After 21 days, the CEM separating the electrode compartments was replaced by an AEM and the MEC was tested at different HRT (Table 1). MEC2 was inoculated with effluent from MEC1 (phase AEM2) and was operated for one month in fed-batch mode on modified M9 medium to establish an electroactive biofilm on the felt before feeding urine. MEC2 was operated at three different HRT to study the effect on the COD removal efficiency and coulombic efficiency (Table 1).

Influent and effluent samples were taken every 2–4 days, filtered over a 0.22 μm Chromafil® Xtra filter (Macherey-Nagel, PA, USA) and stored in the fridge (4 °C) prior to analysis. The coulombic efficiency (CE; in this manuscript defined as the ratio between the real current that was monitored with the potentiostat and the theoretical current calculated based on the COD removal) was calculated with the following equation (Logan et al., 2006).

$$CE [\%] = \frac{100 \times \text{current} [A]}{(\text{COD}_{in} - \text{COD}_{out}) \left[ \frac{\text{g COD}}{\text{L}} \right] \times \text{flow rate} \left[ \frac{\text{L}}{\text{d}} \right] \times \frac{4 \frac{\text{mol e}^-}{\text{mol O}_2} \times 96.485 \frac{\text{C}}{\text{mol e}^-}}{32 \frac{\text{g O}_2}{\text{mol O}_2} \times (24 \times 60 \times 60) \frac{\text{s}}{\text{d}}}}$$

### 2.2.3. MABR operation

The MABR was inoculated with sludge from a urine nitrification reactor (Eawag, Switzerland) and was operated for 10 days in batch mode and for 35 days in continuous mode on a synthetic solution containing (NH<sub>4</sub>)<sub>2</sub>SO<sub>4</sub> as N source (1 g N L<sup>-1</sup>), NaHCO<sub>3</sub> and K<sub>2</sub>HPO<sub>4</sub>. Subsequently, diluted MEC effluent (16% urine) was dosed to the reactor and the loading was gradually increased by increasing the influent flow rate (phase MEC I) (Table 2). On day 66 and 92, the urine concentration was increased to 25% urine (MEC II) and 33% urine (MEC III), respectively, by decreasing the dilution of the MEC effluent. At the end of phase MEC III (day 168), one HF bundle was removed for microbial community analysis and the MABR was fed with a synthetic solution until the start of phase MEC IV. To evaluate the effect of the MEC pre-treatment, the loading was increased until a bulk DO concentration below 0.1 mg O<sub>2</sub> L<sup>-1</sup> was reached in phase MEC IV. Next, the MABR was operated at the same N loading but on raw urine (stabilised with NaOH to prevent urea hydrolysis in the influent) instead of MEC effluent for 56 days (RAW I). In phase RAW II, the air flow rate and recirculation rate were increased to 1.5 L min<sup>-1</sup> and 16.3 L h<sup>-1</sup>, respectively, to

**Table 2**  
**Overview of different operational phases of the membrane-aerated biofilm reactor (MABR).** Averages and standard deviations are presented. Average influent and effluent compositions are reported in SI, Section E.

Phase	MEC I <sup>a</sup>	MEC II	MEC III <sup>b</sup>	MEC IV <sup>b</sup>	RAW I <sup>b</sup>	RAW II	MEC V <sup>b</sup>	MEC VI
Number of HF bundles	3	3	3	2	2	2	2	2
Influent	MEC1 effluent	MEC2 effluent	MEC2 effluent	MEC2 effluent	stabilised urine	stabilised urine	MEC2 effluent	MEC2 effluent
	16.7%	25%	33.3%	33.3%	33.3%	33.3%	33.3%	33.3%
Day	1 <sup>c</sup> - 65	66 - 91	92 - 168	205 - 266	267 - 322	323 - 339	340 - 381	382 - 392
Duration [d]	65	26	77	62	56	17	42	11
Duration (number of HRT)	7.2	4.5	13.4	6.5	6.3	1.8	5.5	1.8
HRT [d]	5.5 ± 0.3	5.8 ± 0.3	5.6 ± 0.2	8.8 ± 0.5	8.8 ± 0.3	9.4 ± 0.3	8.2 ± 0.6	6.2 ± 0.0
N load [mg N d <sup>-1</sup> ]	84 ± 6	109 ± 3	151 ± 18	100 ± 8	102 ± 2	101 ± 3	93 ± 4	125 ± 5
N loading rate <sup>d</sup> [mg N L <sup>-1</sup> d <sup>-1</sup> ]	129 ± 9	168 ± 5	232 ± 28	198 ± 16	202 ± 4	199 ± 5	183 ± 9	247 ± 9
COD load [mg COD d <sup>-1</sup> ]	18 ± 2	22 ± 2	25 ± 5	18 ± 1	101 ± 2	99 ± 2	21 ± 1	27 ± 1
COD loading rate <sup>d</sup> [mg COD L <sup>-1</sup> d <sup>-1</sup> ]	27 ± 3	33 ± 3	38 ± 8	35 ± 3	200 ± 3	196 ± 5	41 ± 2	54 ± 2
NOD <sup>e</sup> [mg O <sub>2</sub> /d <sup>-1</sup> ]	362 ± 25	472 ± 13	653 ± 78	434 ± 35	443 ± 8	434 ± 11	401 ± 19	542 ± 21
BOD for COD oxidation <sup>f</sup> [mg O <sub>2</sub> d <sup>-1</sup> ]	0 ± 0	3 ± 2	3 ± 3	8 ± 1	72 ± 1 <sup>g</sup>	72 ± 2 <sup>g</sup>	9 ± 1	12 ± 1
Total biological oxygen demand (NOD+BOD) [mg O <sub>2</sub> d <sup>-1</sup> ]	362 ± 25	475 ± 16	656 ± 81	442 ± 36	514 ± 9	506 ± 13	409 ± 20	554 ± 21
Average DO [mg O <sub>2</sub> L <sup>-1</sup> ]	4.82 ± 0.40	4.57 ± 0.72	2.65 ± 0.42	0.10 ± 0.12	0.02 ± 0.01	0.03 ± 0.01	0.04 ± 0.14	0.03 ± 0.01
Temperature [°C]	27.1 ± 1.3	25.9 ± 1.5	30.4 ± 1.1	22.5 ± 1.0	22.1 ± 1.0	20.0 ± 0.9	22.7 ± 0.9	23.1 ± 0.8
pH influent	9.1 ± 0.1	9.2 ± 0.1	9.1 ± 0.0	9.2 ± 0.1	11.3 ± 0.1	10.8 ± 0.1	9.1 ± 0.0	9.2 ± 0.0

<sup>a</sup> HRT, N/COD load & loading, oxygen demand and DO are calculated based on data after reaching steady state with a fixed influent flow rate (days 49–65).

<sup>b</sup> HRT, N/COD load & loading and oxygen demand are calculated based on data after the first 3 HRT (steady state).

<sup>c</sup> Day 1 corresponds to the first day that the reactor was operated on MEC effluent (45 days after start-up of the reactor).

<sup>d</sup> The loading was calculated taking into account the total reactor volume (MEC I-III=650 mL, MEC IV-VI and RAW I-II=500 mL).

<sup>e</sup> The Nitrogenous Oxygen Demand (NOD) was estimated assuming 4.33 g O<sub>2</sub> g<sup>-1</sup> N for nitrification.

<sup>f</sup> The Biological Oxygen Demand (BOD) for COD oxidation is estimated assuming that all COD is removed aerobically, consuming 0.8 g O<sub>2</sub> g<sup>-1</sup> COD removed (i.e., cell yield of 0.2).

<sup>g</sup> The BOD for COD oxidation is overestimated in RAW I and RAW II since a part of the COD was removed using nitrate as an electron-acceptor instead of oxygen.

enhance the oxygen mass transfer. Afterwards, the MABR was operated again on MEC effluent at the same N loading and initial air flow rate and recirculation rate (0.65–0.75 L min<sup>-1</sup> and 11 L h<sup>-1</sup>, respectively) (phase MEC V). Between phase RAW II and MEC V, no influent was dosed for two days to allow oxidation of the TAN that accumulated during RAW II. In phase MEC VI, the N loading was further increased.

Influent and effluent samples were taken every 2–4 days, filtered over a 0.22 µm Chromafil® Xtra filter (Macherey-Nagel, PA, USA) and stored in the fridge (4 °C) prior to analysis.

### 2.3. Analytical methods

Ions were analysed on a compact ion chromatograph equipped with a conductivity detector (Metrohm 930 with Metrosep A supp 5-150/4.0 column for anions and Metrohm 761 with Metrosep A supp 5-150/4.0 column for cations, Metrohm, Switzerland). The TAN concentration in the MABR effluent (low concentration) was determined according to the Montgomery reaction (Montgomery and Dymock 1961) with a Tecan infinite plate reader (Infinite® F50 Absorbance Microplate Reader, Tecan Trading AG, Switzerland). Nanocolor tube test kits (Nanocolor® TN220 and Nanocolor® COD160/1500, Macherey-Nagel, PA, USA) were used to measure the total nitrogen (TN) and COD concentration. The electrical conductivity was measured with a conductivity meter (Consort C6010 with a Metrohm 6.0912.110 conductivity probe) and pH measurements were performed with a portable pH meter (C5010, Consort bvba, Belgium).

### 2.4. Microbial community analysis

Samples from both reactors were collected throughout the experiments for microbial community analysis. The different MEC microenvironments (MEC anolyte, graphite granules and/or felt)

were sampled at the end of each experiment (Table 1). One of the MABR bundles (MABR bundle 1) was sacrificed for sequencing after phase MEC III and another bundle (MABR bundle 2) was sampled after MEC VI (Table 2). Biomass from the flocs, fibers, and firmly attached biomass (after scraping off loosely attached biomass from the fibers) were collected. The samples were stored at –20 °C prior to DNA extraction and quality control, performed as described by De Paepe et al. (2017). DNA extracts were sent out to BaseClear BV (Leiden, The Netherlands) for library preparation and sequencing of the V3–V4 region of the 16S rRNA gene on an Illumina MiSeq platform (Illumina, Hayward, CA, US) with Illumina MiSeq v3 chemistry and using the 341F–785R primerpair adopted from Klindworth et al. (2013). The sequence data are available at the NCBI (National Center for Biotechnology Information) database under accession number PRJNA572564. The data was processed with the mothur software package (v.1.40.5) (Schloss et al., 2009) as outlined by De Paepe et al. (2017). OTUs (Operational Taxonomic Units) were defined as a collection of sequences with a length between 393 and 429 nucleotides that were found to be more than 97% similar to one another in the V3–V4 region of their 16S rRNA gene after applying OptiClust clustering (Chen et al., 2013; Schloss and Westcott 2011; Schloss et al., 2009; Wang et al., 2012). Taxonomy was assigned using the silva.nr\_v132 database (Cole et al., 2014; Quast et al., 2013; Wang et al., 2007). The OTU table with taxonomy assignment was loaded into R, version 3.6.1 (2019-07-05), and singletons were removed (McMurdie and Holmes 2014; R Core Team 2016). A Principle Coordinate Analysis (PCoA; package stats 4.3.6.1) was used to explore differences in microbial community composition, which were visualised with ggplot2 version 3.2.1 (Becker et al., 1988; Cailliez 1983; Cox 2001; Gower 1966; Ramette 2007; Wickham 2009). For this purpose, the shared file (including the duplicate samples) was filtered based on the arbitrary cut-offs described by McMurdie and Holmes (2014), whereby OTUs observed in less than 5% of the samples and with

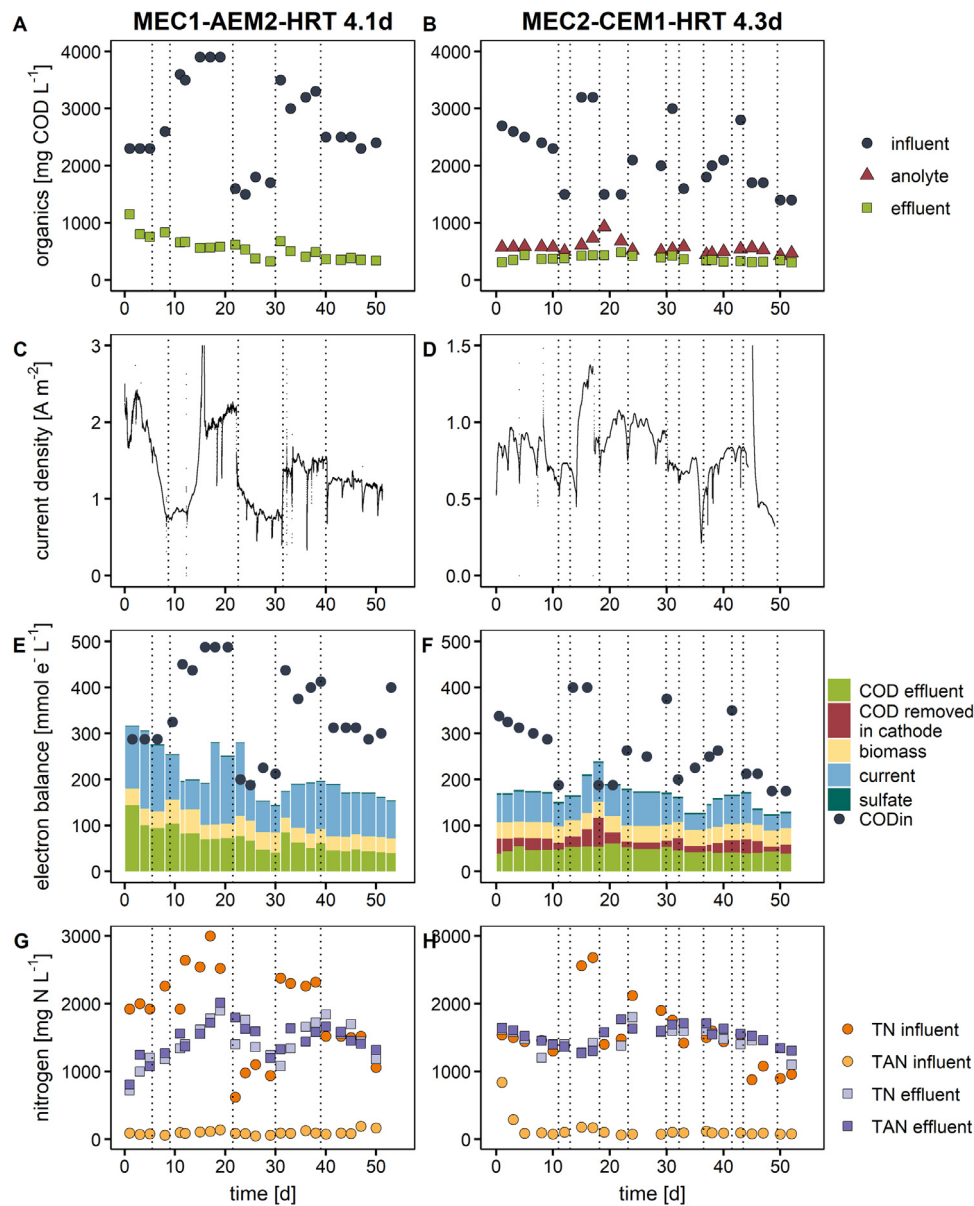


**Fig. 2.** COD removal (A-B), current density (C-D), electron balance (E-F) and nitrogen balance (G-H) of MEC1 operated with an AEM at a HRT of 4.1 days (MEC1-AEM2) and MEC2 operated with a CEM at a HRT of 4.3 days (MEC2-CEM1). Different batches of urine were fed to the MECs, as indicated by the dashed lines on the graphs. The equations used to calculate the electron balance are given in SI Section D.

read counts below 0.5 times the number of samples were removed. The data was rescaled to proportions and the abundance based jaccard dissimilarity matrix was calculated (package *vegan* 2.4–3) (Anderson et al., 2006; Borcard et al., 2011; McMurdie and Holmes 2014; Oksanen et al., 2016). On the genus level, weighted averages of genera abundances were *a posteriori* added to the ordination plot, using the *wascor* function in *vegan* (Oksanen et al., 2016).

### 3. Results

#### 3.1. COD removal, current production, coulombic efficiency and urea hydrolysis in the MEC

The primary goal of the MEC was to remove organics from urine in an energy-efficient way, as to prevent N loss via denitrification in the MABR. Due to the use of different batches of urine, the influent COD concentration and load were varying over time, as exemplified in Fig. 2A and B for MEC1-AEM2 and MEC2-CEM1, respec-

tively. Despite the fluctuating influent COD concentration, the COD concentration in the effluent remained stable. Electroactive bacteria transferred the electrons obtained by COD oxidation to the anode, generating an electric current from anode to cathode. The current density ranged between 0.5 and 2 A m<sup>-2</sup> (membrane projected surface) in all experiments (Table 3), and followed the same pattern as the influent COD concentration, i.e., a high influent COD concentration resulted in a higher current (Fig. 2C-D). Apart from COD removal, urea hydrolysis took place in the MEC, increasing the TAN/TN ratio from <10% (influent) to ~100% (effluent) (Fig. 2G-H, Table 3).

MEC1 was initially operated with a CEM separating the two electrode compartments and achieved COD removal efficiencies around 80% at an HRT of 6.6 days and an average COD loading of  $22.4 \pm 5.3$  g COD m<sup>-2</sup> d<sup>-1</sup> (Table 3, MEC1-CEM). The average current density was  $1.0 \pm 0.3$  A m<sup>-2</sup> (Table 3), which was about 42% of the current that was expected based on the observed COD removal (i.e., coulombic efficiency). Because of the electron flow

**Table 3**

MEC: average COD loading, COD removal efficiency, cell voltage, current density, coulombic efficiency, N balance ( $N_{\text{effluent}}/N_{\text{influent}}$ ), TAN/TN (total ammonia nitrogen/total nitrogen) ratio and pH in the effluent. The large standard deviations are caused by the use of different batches of urine (with a different composition). For MEC2, two HRT, COD removal efficiencies and pH values are reported: the value on the first row is the HRT/COD removal efficiency/pH in the anodic compartment, the value on the second row is the total HRT/COD removal efficiency/pH after passage through the cathodic compartment. Time series data are presented in SI (Figures S2-S3) and Fig. 2 (MEC1-AEM2 and MEC2-CEM1).

	HRT [d]	COD loading [g COD m <sup>-2</sup> d <sup>-1</sup> ]*	COD removal efficiency [%]	anode potential [mV]	cell voltage [mV]	current density [A m <sup>-2</sup> ]*	coulombic efficiency [%]	N balance [%]	TAN/TN [%]	pH
MEC1-CEM	6.6	22.4 ± 5.3	80 ± 7	-350	-713 ± 57	1.0 ± 0.3	42 ± 5	34 ± 6	92 ± 8	8.1 ± 0.2
MEC1- AEM1	6.7	29.4 ± 1.5	86 ± 3	-350	-769 ± 83	1.3 ± 0.2	38 ± 5	81 ± 0	98 ± 4	8.4 ± 0.2
MEC1- AEM2	4.1	32.3 ± 8.8	79 ± 9	-250	-919 ± 93	1.4 ± 0.6	41 ± 21	59 ± 15	103 ± 13	8.7 ± 0.4
MEC1- AEM3	3.7	28.1 ± 8.9	81 ± 8	-250	-907 ± 41	1.3 ± 0.3	46 ± 13	89 ± 21	100 ± 2	9.0 ± 0.2
MEC2- CEM1	4.3	30.6 ± 7.9	73 ± 7	-250	-762 ± 25	0.8 ± 0.2	27 ± 11	98 ± 23	105 ± 9	8.7 ± 0.2
	7.3		81 ± 6							9.4 ± 0.1
MEC2- CEM2	2.5	33.7 ± 5.3	48 ± 4	-250	-781 ± 16	0.8 ± 0.1	36 ± 4	96 ± 15	115 ± 9	9.0 ± 0.1
	4.3		71 ± 5							9.3 ± 0.1
MEC2- CEM3	5.5	19.8 ± 4.9	40 ± 9	-250	-770 ± 27	0.5 ± 0.1	33 ± 18			8.9 ± 0.2
	9.4		68 ± 9							9.3 ± 0.1

\* Membrane projected surface area (100 cm<sup>2</sup>).

from anode to cathode, cations migrated from the anolyte to the catholyte through the CEM to restore the charge balance. As a result, more than 65% of the N was removed from the urine (anolyte) by migration of ammonium. The average pH in the effluent of the anolyte was 8.1, and was affected by the pH of the influent (~11), urea hydrolysis (producing TAN and bicarbonate), proton production by COD oxidation and proton migration through the CEM to the cathodic compartment.

In order to prevent the loss of ammonium by migration, the CEM was replaced by an AEM. The average COD removal efficiency equalled 86% at an HRT of 6.7 days and an average COD loading of 29.4 ± 1.5 g COD m<sup>-2</sup> d<sup>-1</sup> (MEC1-AEM1, Table 3, SI Section C). Next, the HRT was decreased from 6.7 to 4.1 days (MEC1-AEM2) and to 3.7 days (MEC1-AEM3) by decreasing the volume of the anode recirculation bottle and slightly increasing the influent flow (Table 2). Decreasing the HRT did not affect the COD removal efficiency (~79–86%), the current production (~1.3–1.4 A m<sup>-2</sup>) nor the coulombic efficiency (~38–46%), as the COD loading remained similar (Table 3, SI Section C). The effluent pH was higher compared to MEC1-CEM (8.4–9 compared to 8.1) because of the OH<sup>-</sup> migration from the catholyte through the AEM to the anolyte (OH<sup>-</sup> ions are produced at the cathode by water reduction). Despite the replacement of the CEM by an AEM, 11–41% of the N was lost in all experiments with an AEM in MEC1. Because of the high pH (8.4–9), a substantial fraction of TAN was present as ammonia, which can diffuse through the AEM to the cathodic compartment.

Therefore, in MEC2, the effluent of the anodic compartment was directed to the cathodic compartment in order to capture all the N that migrated or diffused through the membrane (CEM). Also the granules were replaced by a single graphite felt to attempt to increase the coulombic efficiency, but the average coulombic efficiency (27%) did not improve (Table 3). Decreasing the HRT in the anodic compartment from 4.3 days to 2.5 days by increasing the influent flow (and thus COD load), resulted in a higher coulombic efficiency (36%) but decreased the COD removal efficiency in the anodic compartment from 73% to 48% (MEC2-CEM2, Table 3). Increasing the HRT to 5.5 days in MEC2-CEM3 did not restore the COD removal in the anodic compartment. At all HRT, the COD in the catholyte was lower than the COD in the anolyte, indicating that additional COD was removed in the cathodic compartment of MEC2 (Table 3, Fig. 2B). MEC2 did not improve the COD removal

and current production, but was successful in preventing N loss from the urine. On average 96–98% of the N in the influent was contained in the effluent. Moreover, by redirecting the urine to the cathodic compartment, all OH<sup>-</sup> that was produced at the cathode was recovered, resulting in a slightly higher effluent pH compared to MEC1 (Table 3).

### 3.2. Nitrification and COD removal in the MABR

The MEC effluent was fed into the MABR to convert TAN into nitrate by nitrification. In the first phase (MEC I, Table 2), the effluent of the MEC was diluted 50%, corresponding to a 16.7% urine solution with a TN concentration of about 760 mg N L<sup>-1</sup> (Fig. 3B and SI Table S3). The load was gradually increased from ~40 mg N d<sup>-1</sup> (day 1) to ~85 mg N d<sup>-1</sup> (day 49–65) by increasing the influent flow, resulting in a decreasing bulk DO concentration due to the increased bacterial activity (Figs. 3A, SI S4). The pH was controlled at 6.85 with NaOH to obtain full nitrification. All N in the influent was present as TAN since urea hydrolysis occurred in the MEC (Fig. 3B). Apart from some accumulation in the first days, the TAN and nitrite concentration in the effluent were both below 10 mg N L<sup>-1</sup> (Fig. 3D). The nitrate concentration in the effluent gradually increased and equalled the TN concentration in the effluent (Fig. 3D). Between days 49 and 65, the nitrate and TN concentration remained stable at ~645 mg N L<sup>-1</sup>, which corresponded to 92–94% of the incoming N concentration (after rescaling the influent concentration to account for the difference in influent and effluent volume caused by the NaOH addition for pH control) (Fig. 3C). The chloride balance equalled 93%, suggesting that steady state might not have been reached yet at the end of the phase. About 150 mg COD L<sup>-1</sup> was present in the influent and effluent, indicating that all (readily) biodegradable COD had been removed in the MEC (HRT of 4.1 d) and the remaining COD was not removed in the MABR (HRT of 5.5 d) (Fig. 3E).

On day 66, the urine concentration was increased to 25% urine (MEC II). As a result, the load increased to ~110 mg N d<sup>-1</sup> (Table 2, SI Fig. S4), and the nitrate and TN concentration in the effluent gradually increased (Fig. 3D), whereas the bulk DO concentration decreased to ~4.6 mg O<sub>2</sub> L<sup>-1</sup> (Fig. 3A). Due to an issue with the pH controller on day 77, acid was added to the reactor resulting in a temporary decrease in nitrate and TN concentration (because of

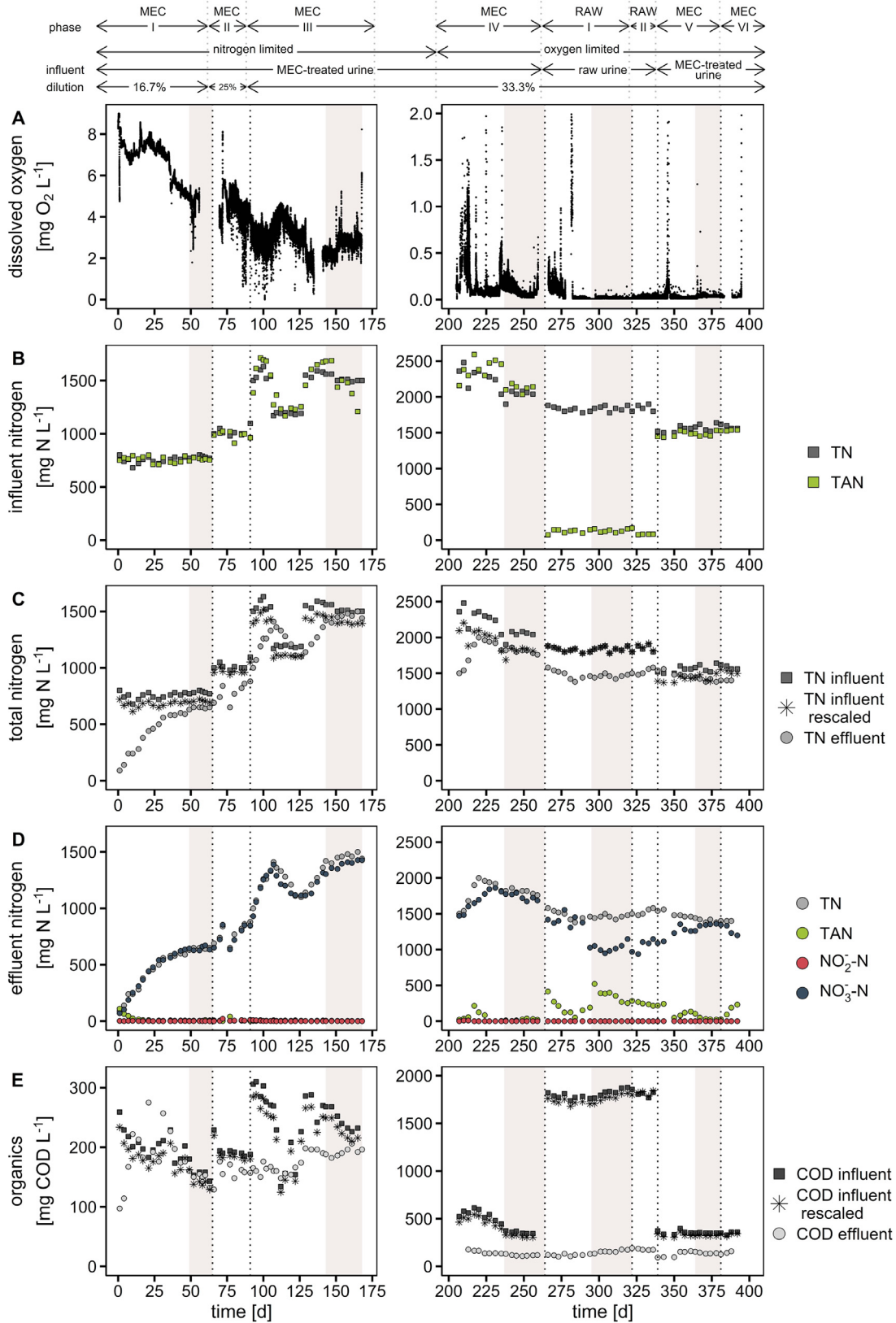


**Fig. 3.** MABR: dissolved oxygen (DO) concentration in the bulk liquid (A), nitrogen speciation in the influent (B), total nitrogen (TN) concentration in the influent and effluent (C), nitrogen speciation in the effluent (D) and COD concentration in the influent and effluent (E). Steady state periods are indicated with a gray background. As the influent and effluent volume were not equal due to the base addition for pH control, the influent concentration was rescaled in plots C and E. The average compositions of influent and effluent in each phase are given in SI Tables S3 and S4.

the dilution with acid) and some TAN accumulation (41 mg TAN L<sup>-1</sup>).

On day 92, the urine concentration was further increased to 33.3% urine (MEC III). The load fluctuated between 130 and 160 mg N d<sup>-1</sup>, due to the use of different batches of MEC effluent with a different N concentration (~1500 mg N L<sup>-1</sup> (day 92–106), ~1200 mg N L<sup>-1</sup> (day 107–128) and ~1500 mg N L<sup>-1</sup> (day 129–168), Fig. 3B, SI Fig. S4). Also the nitrate and TN concentration in the effluent and the bulk DO concentration varied between 1100 and 1500 mg N L<sup>-1</sup> and 2–4 mg O<sub>2</sub> L<sup>-1</sup>, respectively (Fig. 3A,D). The TN concentration in the effluent coincided with the (rescaled) influent, when steady state was reached (day 143–168), whereas the COD concentration in the effluent was ~16% lower than the (rescaled) influent concentration, indicating some COD removal by heterotrophic bacteria in the MABR.

From MEC I to III, the bulk DO concentration dropped because of the increasing influent flow rate (in MEC I) or increased urine concentration (MEC II & III), but was still higher than 2 mg O<sub>2</sub> L<sup>-1</sup>. Therefore, in MEC IV, the load was further increased until a DO below 0.2 mg O<sub>2</sub> L<sup>-1</sup> was reached, at a load of ~100 mg N d<sup>-1</sup>. This load was lower compared to the load during MEC II–III, since the MABR, after sacrificing one HF bundle for microbial community analysis, only consisted of two HF bundles. Apart from some TAN accumulation at the start (day 207–224), full nitrification was obtained and no N losses were observed (rescaled TN influent coincided with TN effluent, Fig. 3C–D) at an average bulk DO concentration of 0.1 mg O<sub>2</sub> L<sup>-1</sup>. The COD concentration in the effluent (116 ± 7 mg COD L<sup>-1</sup>) was 63% lower than the (rescaled) concentration in the influent (355 ± 13 mg COD L<sup>-1</sup>).

In the next phase (RAW I), the MABR was operated at the same N load (~100 mg N d<sup>-1</sup>) but on diluted raw urine (33.3%), which was stabilised (i.e., NaOH was added to obtain a pH > 11, in order to inhibit urea hydrolysis in the influent) but not treated in a MEC. Unlike the MEC effluent in which all N was present as TAN, organic N was the predominant N species in the raw urine (Fig. 3B). Only ~7% of the TN in the influent (~1850 mg N L<sup>-1</sup>) was TAN (~135 mg N L<sup>-1</sup>), requiring urea hydrolysis in the MABR. Furthermore, without pre-treatment in the MEC, the COD concentration in the influent was substantially higher (1850 mg COD L<sup>-1</sup> compared to only 355 mg COD L<sup>-1</sup> in MEC IV) (Fig. 3E). The COD concentration in the effluent did not increase (Fig. 3E), thus the MABR was able to remove all (readily) biodegradable COD (91% of the incoming COD). However, the higher COD load and oxygen demand hampered nitrification, with oxygen becoming a limiting substrate, resulting in partial nitrification. The effluent contained 20–25% TAN and 70–75% nitrate from day 297 onwards (Fig. 3D). The oxygen limitation furthermore gave rise to denitrification, with a TN concentration in the effluent ~18% lower than the (rescaled) TN concentration in the influent.

On day 323, the air flow rate and recirculation rate were increased to enhance the oxygen mass transfer through the hollow fiber membranes (RAW II). As a result, the TAN concentration in the effluent decreased (14% of the TN concentration), while the TN concentration in the effluent slightly increased (83.4% of the rescaled TN concentration) (Fig. 3C–D).

Subsequently, the MABR was operated again on MEC effluent at the same N load of 100 mg N d<sup>-1</sup> (MEC V), reverting successfully to full nitrification without N loss (Fig. 3C–D).

In a last phase (MEC VI), the MABR was operated on MEC effluent but at a load of 125 mg N d<sup>-1</sup>, resulting in DO limitation and TAN accumulation, but without N loss, showing robustness against variable N loading (Fig. 3C–D).

### 3.3. Microbial community composition of MEC and MABR

Amplicon 16S rRNA gene Illumina sequencing and principle coordinate analyses (SI Figs. S11, S16 and S17) revealed that the MEC

and MABR units were characterised by very distinct and diverse microbial communities (Fig. 4–SI Figs. S7–S17). This divergence in the first place stems from the different inocula that were introduced into the MEC and MABR. MEC1 was inoculated with effluent originating from an active MEC (fed with fermenter supernatant) and effluent from MEC1 was used to inoculate MEC2. The MABR was inoculated with sludge from a urine nitrification reactor operated at Eawag (Switzerland). The communities were further shaped by the different conditions (anoxic versus oxic, high versus low COD loading, different pH and conductivity) resulting in stable communities adapted to carry out the particular biological processes (i.e., anodic COD oxidation versus nitrification) in both MEC and MABR, even despite the influx of MEC effluent in the latter.

At phylum and family level, the MEC was rich in *Proteobacteria* (~50%, mainly *Burkholderiaceae*, *Geobacteraceae* and *Pseudomonadaceae*), *Bacteroidetes* (~25%, including *Lentimicrobiaceae* and *Dysgonomonadaceae*) and *Firmicutes* (~25%, mainly *Carnobacteriaceae* and *Clostridiaceae*) (SI Figs. S7–S8), whereas the MABR was dominated by *Bacteroidetes* (~40%, amongst others *Chitinophagaceae* and *Saprosiraceae*), *Proteobacteria* (~30%, including *Burkholderiaceae* and *Nitrosomonadaceae*) and *Actinobacteria* (~15%, e.g., *Nocardiaceae*) (SI Figs. S12–S13).

At genus level, the MEC community was dominated by *Geobacter*, *Pseudomonas*, *Arcobacter* and *Comamonas*, genera known to comprise electroactive bacteria (Bond et al., 2002; Logan et al., 2019; Rabaey et al., 2004; Xing et al., 2010) (SI Figs. S9–S10). Furthermore, alkaliphilic genera (*Alcaligenes* and *Alkalibacter*), *Thiopseudomonas*, *Lentimicrobiaceae*, *Proteiniphilum*, and *Tissierella* were abundant (pH was ~9 in MEC). Interestingly, a member of the *Tissierella* genus (*Tissierella creatinophila*) is able to grow on creatinine (one of the main COD compounds in urine) as sole carbon and energy source and degrades creatinine to acetate, monomethylamine, ammonia and carbon dioxide (Harms et al., 1998).

Although their relative abundance varied strongly across samples, this core set of genera dominated the microbial community throughout time regardless of modifications in reactor configuration and operation, except for *Synergistaceae* which were abundant in the inoculum (~15%) and initially also in the MEC (MEC1–CEM), but almost disappeared afterwards (SI Figure S8). Besides the absence of a temporal effect, there were no consistent differences in microbial community between the microenvironments (i.e., anolyte, felt or granules) (Fig. 4, SI Figs. S7–S11). Even samples taken at the same moment from the graphite felt used in MEC2–CEM3 were different. This indicates that stochastic effects are responsible for the observed differences between samples and microenvironments and that there is no niche preference (no specific association of certain community members with the different microenvironments).

While (strictly) anaerobic genera prevailed in the MEC, the MABR was dominated by aerobic genera, including *Nitrosomonas*, *Moheibacter* and *Gordonia* (Fig. 4). About 5–10% of the community in the MABR was a member of the ammonium oxidizing genus *Nitrosomonas*. *Nitrosospira*, another AOB genus, was also present but at lower relative abundances (<0.5%). Members of known nitrite oxidizing genera (*Nitrobacter*, *Nitrospira*) were not retrieved, even though nitratation occurred in the MABR.

Samples originating from bundles 1 and 2 clustered separately in a principle coordinate analysis (PCoA) analysis at genus level and were clearly different from the inoculum (SI Fig. S16). Bundle 1 was harvested after MEC III (operation without oxygen limitation), whereas bundle 2 was harvested at the end of the experiment (after MEC VI), including the period with oxygen limitation and operation on raw urine with a high COD concentration and urea as main N source. Bundle 2 was more enriched in PHOS-HE36 (member of *Ignavibacteria*) and UTCFX1 (belonging to the *Anaero-*

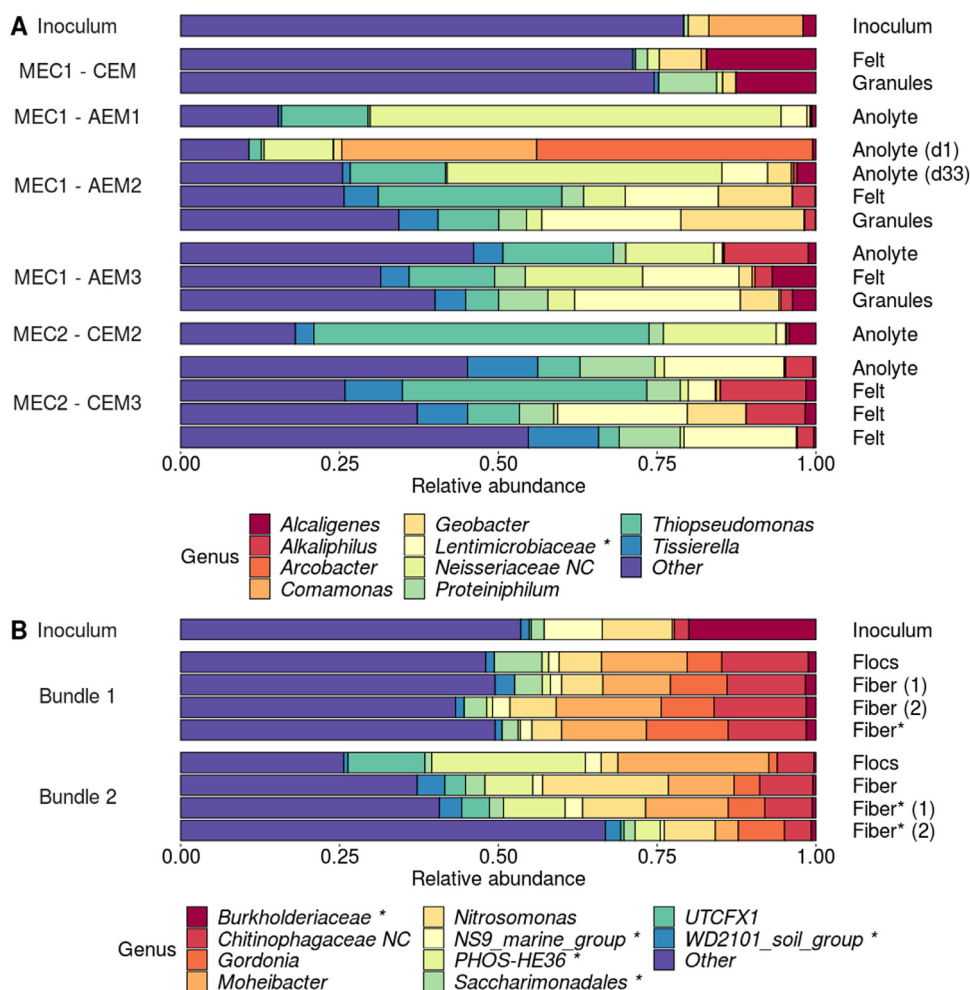


**Fig. 4.** Composition of the microbial communities at genus level (where possible) of the microbial electrolysis cell (MEC, A) and membrane-aerated biofilm reactor (MABR, B). For the MEC, a distinction was made between biomass present in the anolyte, on the felt or on the granules. All samples were taken at the end of the experiment (except 'Inoculum' and 'Anolyte (d1)', taken on the first day) (Table 1). For the MABR, a distinction was made between biomass flocs in the bundle ('flocs'), biomass on the fibers ('fibers') and firmly attached biomass on the fibers after scraping off the loosely attached biomass ('fiber\*'). Bundle 1 and 2 were sampled after Phase MEC III and MEC VI, respectively (Table 2). The numbers between the brackets indicate duplicates. The relative abundance of the ten most abundant genera is shown. Taxa that could not be classified at genus level are specified at family level followed by \*. Uncultured bacteria are indicated by 'NC' (not cultured).

lineaceae), probably as a result of the low DO concentration and higher COD load.

## 4. Discussion

### 4.1. The MEC reached high COD removal efficiencies, yet converted only 25–45% of the removed COD to current

Urine was pre-treated in a MEC to remove organics in an energy-friendly manner as to enable full N recovery in the MABR. However, due to ammonium migration and ammonia diffusion through the membrane, up to 65% of the N was lost in MEC1. This issue was solved in MEC2, by directing the effluent of the anodic compartment through the cathodic compartment. Both MEC1 and MEC2 achieved up to 80–85% COD removal with HRTs between 4 and 7 days. Most studies on urine treatment in continuously fed bio-electrochemical systems (i.e., MEC and MFC) report lower COD removal efficiencies, ranging from ~10% to 46% (SI Section J). These studies mostly focus on energy or TAN recovery, and therefore apply a low HRT (<1d), presumably causing the lower COD removal. Only Walter et al. (2018) obtained a high COD removal efficiency (88%) at a relatively low HRT of 44 h, but the coulombic efficiency was <4%, indicating that most of the COD

was removed by other mechanisms than bio-anodic oxidation. In our study, fresh urine was used to feed the MEC, while most studies in literature use stored urine. Fresh urine is composed of complex organic molecules (including long-chain organic acids, creatinine, amino acids and carbohydrates), whereas in stored urine, a significant fraction of the complex organic molecules are already hydrolysed/fermented into acetate and other smaller molecules, which are easier substrates because they can be directly converted into electricity by electroactive bacteria (Barbosa et al., 2019; Larsen et al., 2013).

The MEC operation should be further optimised in order to increase the coulombic efficiency, because, despite the high COD removal efficiencies, a low current output was obtained. Only about 27–46% of the COD removed was converted into current, indicating the presence of competing electron sinks (e.g., alternative electron acceptors such as nitrate and sulfate, biomass production, competition with non-electroactive bacteria for COD). The coulombic efficiencies in bio-electrochemical systems fed with urine reported in literature range from 2% to 97%, but are usually lower than 30% (SI Section J). Tice and Kim (2014) reported that the high sulfate concentration in human urine favored acetate-oxidizing and H<sub>2</sub>-oxidizing sulfate reducing bacteria, greatly diminishing the coulombic efficiency (due to COD consumption by

acetate-oxidizing sulfate reducers) and energy recovery (due to H<sub>2</sub> consumption by H<sub>2</sub>-oxidizing sulfate reducers) in a MEC coupled with an IEM stack. In an attempt to identify the reason for the low coulombic efficiency in our experiments, an electron balance was made in Fig. 2E-F and SI Section D. About 20% of the incoming COD (and electrons) was not converted and was still present in the effluent. A part of the electrons generated by COD oxidation was incorporated into biomass. This fraction was estimated at ~10% based on the volatile suspended solids concentration in the MEC. The fraction of electrons going to alternative electron acceptors was minimal, since the nitrate and oxygen concentration were negligible and only a small amount of sulfate disappeared (15–33 mg SO<sub>4</sub> L<sup>-1</sup> in MEC1 and 57–177 mg SO<sub>4</sub> L<sup>-1</sup> in MEC2, compared to 1–2.3 g COD L<sup>-1</sup>). As demonstrated in Fig. 2E-F, the electron balance could not be closed by adding up all the abovementioned electron sinks. Fermentation and methanogenesis are also known to decrease the coulombic efficiencies in bio-electrochemical systems because of substrate consumption via these metabolic pathways (Logan et al., 2006). In general, methanogens are highly sensitive to free ammonia (FA) (Kuntke et al., 2018; Sprott and Patel 1986; Yenigün and Demirel 2013), which makes methanogenesis unlikely in our MEC, because of the high pH and high N concentration (>750 mg FA L<sup>-1</sup>). The headspace of the anolyte recirculation vessel was sampled two times and no methane was detected with gas chromatography. Fermentation is more likely because of the presence of fermentable compounds in urine (e.g., lactate and glucose) (Barbosa et al., 2019). When complex organic molecules are fermented into simpler organic molecules (e.g., acetate), part of the COD is converted into hydrogen gas, which is a poor substrate for electroactive bacteria but a good electron donor for hydrogenotrophic methanogens, using bicarbonate as a terminal electron acceptor (Lee and Rittmann 2010; Lee et al., 2008). Further decreasing the HRT or adapting the anode potential could potentially favor electrogenesis compared to fermentative or methanogenic bacteria and thereby increase the coulombic efficiency. Analysing the different COD compounds in the influent and effluent could also gain new insights.

#### 4.2. Upstream bio-anodic COD oxidation effectively prevented denitrification in the MABR

The MEC effluent was fed into a nitrification MABR to convert all TAN into nitrate. Overall, full nitrification (effluent TAN and NO<sub>2</sub><sup>-</sup>-N <5 mg N L<sup>-1</sup>) without N loss was obtained when the MABR was operated on MEC effluent at N loads up to 100 mg N d<sup>-1</sup> and bulk DO levels as low as 0.1 mg O<sub>2</sub> L<sup>-1</sup>. The COD concentration in the MABR effluent was slightly lower than the influent concentration, indicating some COD removal. Yet, the oxygen demand for COD oxidation was less than 2% of the total oxygen demand (Table 2). In MEC IV, about ~160 mg O<sub>2</sub> L<sup>-1</sup> was consumed for COD oxidation (assuming that all COD was aerobically removed consuming 0.8 g O<sub>2</sub> g<sup>-1</sup> COD removed), while more than 7800 mg O<sub>2</sub> L<sup>-1</sup> was required for nitrification (assuming that 4.33 g of oxygen is consumed per g of nitrate-N produced). Only in case of overloading (in MEC VI), TAN accumulated, but no N losses were observed.

In contrast, feeding the MABR directly with raw urine yielded TAN accumulation and N loss at a N load of 100 mg N d<sup>-1</sup> due to the high COD influx in the MABR. The nitrification oxygen demand (NOD) was in line with MEC IV, whereas the oxygen demand for COD oxidation was significantly higher (72 mg O<sub>2</sub> d<sup>-1</sup> compared to <10 mg O<sub>2</sub> d<sup>-1</sup>) (Table 2). Although the oxygen demand for COD oxidation was less than 15% of the total oxygen demand, the increase in oxygen demand for COD oxidation led to oxygen limitation, resulting in TAN accumulation and N loss due to denitrification. It was estimated that about 70% of the COD removed

was removed via denitrification, based on the amount of N that was lost and assuming a COD/N ratio of 3.6 (cell yield of 0.2).

Interestingly, TAN (and not nitrite) accumulated in case of oxygen limitation, whereas many studies report nitrite build-up under DO limited conditions (Feng et al., 2008; Udert et al., 2003a; Udert and Wachter 2012). Generally, NOB have a lower affinity to oxygen than AOB (Udert et al., 2003a), resulting in nitrite accumulation at low DO concentrations.

#### 4.3. Both MEC and MABR showed robustness against fluctuating loading rates and operational conditions

Both the MEC and MABR were challenged with various loading rates and operational scenarios. The COD loading in the MEC highly fluctuated because of the use of different urine batches (with a different COD concentration) and because different HRT were tested. Despite these fluctuations in influent composition and loading, the influent COD concentration in the effluent remained stable, demonstrating the robustness of the MEC. Also the MABR could handle different N and COD concentrations and loads. After start-up, the N load was gradually increased from ~40 mg N d<sup>-1</sup> to ~150 mg N d<sup>-1</sup> (Table 2, Fig. S4), corresponding with volumetric loading rates of 60–230 mg N L<sup>-1</sup> d<sup>-1</sup> when the total MABR volume is taken into account or 150–560 mg N L<sup>-1</sup> d<sup>-1</sup> when only the active volume (i.e., total volume of the hollow fiber modules) is considered. A nitrification activity test (presented in Section G of SI) demonstrated that the mixed liquor in the recirculation vessels and loop was not active. In MEC IV and VI, the load was further increased to 100 mg N d<sup>-1</sup> (200 or 560 mg N L<sup>-1</sup> d<sup>-1</sup>) and 125 mg N d<sup>-1</sup> (250 or 700 mg N L<sup>-1</sup> d<sup>-1</sup>), respectively. By shifting the influent from MEC effluent to raw urine, the COD concentration and load increased from 350 to 1850 mg COD L<sup>-1</sup> and from 20 to 100 mg COD d<sup>-1</sup>, respectively. More than 90% of the COD could be removed, maintaining the COD concentration in the effluent <200 mg COD L<sup>-1</sup>. Also, after the period on raw urine with N loss and TAN accumulation, the MABR performance could be reverted successfully to full nitrification without N loss. All these observations illustrate the robustness of the MABR.

#### 4.4. MEC-MABR integration not only prevents N losses but also reduces the overall oxygen demand, increases the alkalinity and enables energy efficient COD removal

Removing the COD prior to membrane-aerated nitrification proved to be key in preventing N losses through denitrification and allowed MABR operation at a high urine loading rate, reducing the required reactor volume. It also minimized biomass production in the MABR since less substrate (COD) was available to the heterotrophs. Bio-anodic COD removal has some clear advantages compared to other biological COD removal processes, for example aerobic COD removal in another MABR. Firstly, there is no oxygen requirement for bio-anodic COD oxidation, whereas aerobic COD removal from urine would consume ~4–8 mg O<sub>2</sub> L<sup>-1</sup> of urine. Secondly, energy can be recovered from the organics, as hydrogen gas (MEC) or electricity (MFC), although this should be further optimized as discussed in Section 4.1. Thirdly, OH<sup>-</sup> production at the cathode increases the alkalinity of the urine, thereby reducing the base demand for full nitrification in the MABR.

#### 4.5. Closing the nitrogen cycle on Earth and in Space

By treatment in the MEC and MABR, fresh real human urine is transformed into a stable nitrate-rich, COD-low nutrient solution, which was demonstrated to be suitable for plant and microalgae cultivation by Coppens et al. (2016) and Feng et al. (2007). Using processed urine as a nutrient source for protein production could

reduce the need for synthetic fertilizers and the related environmental pollution, resulting in a more sustainable nitrogen cycle on Earth. Separate collection and treatment of urine also facilitates wastewater treatment (Wilsenach and van Loosdrecht 2003). Due to the NaOH addition for alkalisation (to prevent urea hydrolysis during storage) and for full nitrification, the sodium concentration in the urine increased by a factor of ~3, which might cause sodium toxicity in plants. To prevent sodium addition, NaOH could be substituted by KOH or an electrochemical cell could be used to supply hydroxide ions as demonstrated by De Paepe et al. (2020).

As the oxidation of COD and N is not based on bubble-dependent gas/liquid mass transfer, the concept is compatible with reduced gravity conditions and can therefore be integrated in regenerative life support systems. On long-term deep-Space missions (e.g., to Mars) and Space habitation, resupply from Earth becomes practically impossible because of the long distance and duration (Clauwaert et al., 2017). Therefore, these missions will rely on a regenerative life support system to produce water, food and oxygen from waste streams, such as urine. In MELISSA, the regenerative life support system program from ESA, urine is treated by nitrification, followed by cyanobacteria and higher plant cultivation (Gòdia et al., 2002). With the survival of nitrifiers demonstrated in low Earth orbit (Lindeboom et al., 2018), the next development step would be to test a urine nitrification MABR in such conditions. As a compact, robust, highly nitrogen- and energy-efficient technology train, the MEC-MABR system could be of interest. Application in a reduced gravity environment would, however, require the use of a gas diffusion air cathode in the MEC (to prevent the production of hydrogen gas, which would be difficult to separate from the liquid in reduced gravity).

## 5. Conclusions

- Upstream bio-anodic COD oxidation effectively prevented denitrification in the MABR. Full nitrification without TAN and nitrite accumulation and without N loss was obtained when the MABR was operated on MEC effluent, whereas denitrification and partial nitrification occurred when the MABR was operated on raw urine at the same N loading rate.
- The MEC allows to operate the MABR at a high loading rate, reduces the oxygen demand for COD oxidation, limits biomass production in the MABR, increases the urine alkalinity and can recover some energy from the organics.
- MEC operation should be further optimized in order to increase the coulombic efficiency, as only about 25–45% of the COD removed was converted into current. Other electron sinks should be identified in order to identify the COD gap and improve the conversion of chemical energy into electrical energy.
- This two-stage process yields a stable nitrate-rich nutrient solution, suitable for plant and microalgae cultivation. As gravity-independent, highly nitrogen- and energy-efficient technology train, the concept can be useful for MELISSA and other regenerative life support systems.

## Declaration of Competing Interest

None.

## Acknowledgments

This article has been made possible through the authors' involvement in the MELISSA project, ESA's life support system research program (<https://www.melissafoundation.org/>).

The authors would like to acknowledge i) the MELISSA foundation to support J.D.P. via the POMPI (Pool Of MELISSA PhD) program, ii) the Research Foundation Flanders (FWO Vlaanderen)

to support K.D.P. (EOS Research project nr. 30770923, project title: Quantitative profiling in applied gut microbiome research, acronym: MiQuant), iii) Ghent University Bijzonder Onderzoeksfonds to support K.R. (GOA grant BOF2019/GOA/026/L), iv) Kai Udert from Eawag (Switzerland) for providing urine nitrification culture, v) Celine Bauwens and Arne Govaert for their help with reactor operation and sample analyses.

## Supplementary material

Supplementary material associated with this article can be found, in the online version, at doi:10.1016/j.watres.2020.116223.

## References

- Anderson, M.J., Ellingsen, K.E., McArdle, B.H., 2006. Multivariate dispersion as a measure of beta diversity. *Ecol. Lett.* 9 (6), 683–693.
- Barbosa, S.G., Rodrigues, T., Peixoto, L., Kuntke, P., Alves, M.M., Pereira, M.A., Ter Heijne, A., 2019. Anaerobic biological fermentation of urine as a strategy to enhance the performance of a microbial electrolysis cell (MEC). *Renew. Energy* 139, 936–943.
- Becker, R.A., Chambers, J.M., Wilks, A.R., 1988. *The New S Language: a Programming Environment for Data Analysis and Graphics*. Wadsworth and Brooks/Cole Advanced Books & Software.
- Bond, D.R., Holmes, D.E., Tender, L.M., Lovley, D.R., 2002. Electrode-reducing microorganisms that harvest energy from marine sediments. *Science* 295 (5554), 483–485.
- Borcard, D., Gillet, F., Legendre, P., 2011. *Numerical Ecology with R*. Springer Science.
- Cailliez, F., 1983. The analytical solution of the additive constant problem. *Psychometrika* 48 (2), 305–308.
- Casey, E., Glennon, B., Hamer, G., 1999. Review of membrane aerated biofilm reactors. *Resour. Conserv. Recycl.* 27 (1), 203–215.
- Chen, R.D., Semmens, M.J., LaPara, T.M., 2008. Biological treatment of a synthetic space mission wastewater using a membrane-aerated, membrane-coupled bioreactor (M2BR). *J. Ind. Microbiol. Biotechnol.* 35 (6), 465–473.
- Chen, W., Zhang, C.K., Cheng, Y., Zhang, S., Zhao, H., 2013. A comparison of methods for clustering 16S rRNA sequences into OTUs. *PLoS ONE* 8 (8), e70837.
- Chen, L.P., Yang, X.X., Tian, X.J., Yao, S., Li, J.Y., Wang, A.M., Yao, Q.A., Peng, D.C., 2017. Partial nitrification of stored source-separated urine by granular activated sludge in a sequencing batch reactor. *AMB Express* 7, 1–10.
- Christenson, D., Sevanthi, R., Morse, A., Jackson, A., 2018. Assessment of Membrane-Aerated Biological Reactors (MABRs) for integration into space-based water recycling system architectures. *Gravitational Space Res.* 6, 12–27.
- Clauwaert, P., Muys, M., Alloul, A., De Paepe, J., Luther, A., Sun, X.Y., Ilgrande, C., Christiaens, M.E.R., Hu, X.N., Zhang, D.D., Lindeboom, R.E.F., Sas, B., Rabaey, K., Boon, N., Ronsse, F., Geelen, D., Vlaeminck, S.E., 2017. Nitrogen cycling in Bioregenerative Life Support Systems: challenges for waste refinery and food production processes. *Progr. Aerosp. Sci.* 91, 87–98.
- Cole, J.R., Wang, Q., Fish, J.A., Chai, B.L., McGarrell, D.M., Sun, Y.N., Brown, C.T., Porras-Alfaro, A., Kuske, C.R., Tiedje, J.M., 2014. Ribosomal database project: data and tools for high throughput rRNA analysis. *Nucl. Acids Res.* 42 (D1), D633–D642.
- Coppens, J., Lindeboom, R., Muys, M., Coessens, W., Alloul, A., Meerbergen, K., Lievens, B., Clauwaert, P., Boon, N., Vlaeminck, S.E., 2016. Nitrification and microalgae cultivation for two-stage biological nutrient valorization from source separated urine. *Bioresour. Technol.* 211, 41–50.
- Côté, P., Bersillon, J.-L., Huyard, A., Faup, G., 1988. Bubble-free aeration using membranes: process analysis. *J. (Water Pollut. Control Federat.)* 60 (11), 1986–1992.
- Cox, T.F., 2001. Multidimensional scaling used in multivariate statistical process control. *J. Appl. Stat.* 28 (3–4), 365–378.
- Feng, D.L., Wu, Z.C., Wang, D.H., 2007. Effects of N source and nitrification pretreatment on growth of *Arthrospira platensis* in human urine. *J. Zhejiang Univ.-Sci. A* 8 (11), 1846–1852.
- Feng, D.L., Wu, Z.C., Xu, S.H., 2008. Nitrification of human urine for its stabilization and nutrient recycling. *Bioresour. Technol.* 99 (14), 6299–6304.
- Fumasoli, A., Etter, B., Skerkele, B., Morgenroth, E., Udert, K.M., 2016. Operating a pilot-scale nitrification/distillation plant for complete nutrient recovery from urine. *Water Sci. Technol.* 73 (1), 215–222.
- Gao, Y., Sun, D., Wang, H., Lu, L., Ma, H., Wang, L., Ren, Z.J., Liang, P., Zhang, X., Chen, X., Huang, X., 2018. Urine-powered synergy of nutrient recovery and urine purification in a microbial electrochemical system. *Environ. Sci.* 4 (10), 1427–1438.
- Gòdia, F., Albiol, J., Montesinos, J.L., Pérez, J., Creus, N., Cabello, F., Mengual, X., Monras, A., Lasseur, C., 2002. MELISSA: a loop of interconnected bioreactors to develop life support in Space. *J. Biotechnol.* 99 (3), 319–330.
- Gong, Z., Yang, F., Liu, S., Bao, H., Hu, S., Furukawa, K., 2007. Feasibility of a membrane-aerated biofilm reactor to achieve single-stage autotrophic nitrogen removal based on Anammox. *Chemosphere* 69 (5), 776–784.
- Gower, J.C., 1966. Some distance properties of latent root and vector methods used in multivariate analysis. *Biometrika* 53 325–8.

- Guo, K., Freguia, S., Dennis, P.G., Chen, X., Donose, B.C., Keller, J., Gooding, J.J., Rabaey, K., 2013. Effects of surface charge and hydrophobicity on anodic biofilm formation, community composition, and current generation in bioelectrochemical systems. *Environ. Sci. Technol.* 47 (13), 7563–7570.
- Harms, C., Schleicher, A., Collins, M.D., Andreesen, J.R., 1998. *Tissierella creatinophila* sp. nov., a gram-positive, anaerobic, non-spore-forming, creatinine-fermenting organism. *Int. J. Syst. Bacteriol.* 48 (Pt 3), 983–993.
- Ieropoulos, I., Greenman, J., Melhuish, C., 2012. Urine utilisation by microbial fuel cells; energy fuel for the future. *Phys. Chem. Chem. Phys.* 14 (1), 94–98.
- Ieropoulos, I.A., Stinchcombe, A., Gajda, I., Forbes, S., Merino-Jimenez, I., Pasternak, G., Sanchez-Herranz, D., Greenman, J., 2016. Pee power urinal – microbial fuel cell technology field trials in the context of sanitation. *Environ. Sci. 2* (2), 336–343.
- Jackson, W.A., Morse, A., McLamore, E., Wiesner, T., Xia, S., 2009. Nitrification-denitrification biological treatment of a high-nitrogen waste stream for water-reuse applications. *Water Environ. Res.* 81 (4), 423–431.
- Jiang, F., Chen, Y., Mackey, H.R., Chen, G.H., van Loosdrecht, M.C.M., 2011. Urine nitrification and sewer discharge to realize in-sewer denitrification to simplify sewage treatment in Hong Kong. *Water Sci. Technol.* 64 (3), 618–626.
- Klindworth, A., Pruesse, E., Schweer, T., Peplies, J., Quast, C., Horn, M., Glockner, F.O., 2013. Evaluation of general 16S ribosomal RNA gene PCR primers for classical and next-generation sequencing-based diversity studies. *Nucl. Acids Res.* 41 (1).
- Kuntke, P., Sleutels, T.H.J.A., Rodríguez Arredondo, M., Georg, S., Barbosa, S.G., ter Heijne, A., Hamelers, H.V.M., Buisman, C.J.N., 2018. (Bio)electrochemical ammonia recovery: progress and perspectives. *Appl. Microbiol. Biotechnol.* 102 (9), 3865–3878.
- Kuntke, P., Sleutels, T.H.J.A., Saakes, M., Buisman, C.J.N., 2014. Hydrogen production and ammonium recovery from urine by a Microbial Electrolysis Cell. *Int. J. Hydrogen Energy* 39 (10), 4771–4778.
- Kuntke, P., Śmiech, K.M., Bruning, H., Zeeman, G., Saakes, M., Sleutels, T.H.J.A., Hamelers, H.V.M., Buisman, C.J.N., 2012. Ammonium recovery and energy production from urine by a microbial fuel cell. *Water Res.* 46 (8), 2627–2636.
- Kuntke, P., Zamora, P., Saakes, M., Buisman, C.J.N., Hamelers, H.V.M., 2016. Gas-permeable hydrophobic tubular membranes for ammonia recovery in bio-electrochemical systems. *Environ. Sci. 2* (2), 261–265.
- Larsen, T.A., Udert, K.M., Lienert, J., 2013. *Source Separation and Decentralization for Wastewater Management*. IWA Publishing.
- Ledezma, P., Jermakka, J., Keller, J., Freguia, S., 2017. Recovering nitrogen as a solid without chemical dosing: bio-electroconcentration for recovery of nutrients from urine. *Environ. Sci. Technol. Lett.* 4 (3), 119–124.
- Lee, H.-S., Rittmann, B.E., 2010. Significance of biological hydrogen oxidation in a continuous single-chamber microbial electrolysis cell. *Environ. Sci. Technol.* 44 (3), 948–954.
- Lee, H.S., Parameswaran, P., Kato-Marcus, A., Torres, C.I., Rittmann, B.E., 2008. Evaluation of energy-conversion efficiencies in microbial fuel cells (MFCs) utilizing fermentable and non-fermentable substrates. *Water Res.* 42 (6–7), 1501–1510.
- Lindeboom, R.E.F., Ilgrande, C., Carvajal-Arroyo, J.M., Coninx, I., Van Hoey, O., Roume, H., Morozova, J., Udert, K.M., Sas, B., Paille, C., Lasseur, C., Ilyin, V., Clauwaert, P., Leys, N., Vlaeminck, S.E., 2018. Nitrogen cycle microorganisms can be reactivated after Space exposure. *Sci. Rep.* 8 (1), 13783.
- Logan, B.E., Hamelers, B., Rozendal, R., Schröder, U., Keller, J., Freguia, S., Aelterman, P., Verstraete, W., Rabaey, K., 2006. *Microbial Fuel Cells: Methodology and Technology*. *Environ. Sci. Technol.* 40 (17), 5181–5192.
- Logan, B.E., Rossi, R., Ragab, A., Saikaly, P.E., 2019. Electroactive microorganisms in bioelectrochemical systems. *Nat. Rev. Microbiol.* 17 (5), 307–319.
- Mackey, H.R., Chen, Y., Chen, G.H., van Loosdrecht, M.C.M., 2010. *Nitrification of Source Separated Urine in a Sequencing Batch Reactor*. IWA Publishing, London.
- Martin, K.J., Nerenberg, R., 2012. The membrane biofilm reactor (MBfR) for water and wastewater treatment: principles, applications, and recent developments. *Bioresour. Technol.* 122, 83–94.
- Maurer, M., Pronk, W., Larsen, T.A., 2006. Treatment processes for source-separated urine. *Water Res.* 40 (17), 3151–3166.
- McMurdie, P.J., Holmes, S., 2014. Waste not, want not: why rarefying microbiome data is inadmissible. *PLoS Comput. Biol.* 10 (4), e1003531.
- Merino-Jimenez, I., Celorrio, V., Fermin, D.J., Greenman, J., Ieropoulos, I., 2017. Enhanced MFC power production and struvite recovery by the addition of sea salts to urine. *Water Res.* 109, 46–53.
- Meyer, C.E., Pensinger, S., Pickering, K.D., Barta, D., Shull, S.A., Vega, L.M., Christenson, D. and Jackson, W.A. (2015) *Rapid Start-up and Loading of an Attached Growth, Simultaneous Nitrification/Denitrification Membrane Aerated Bioreactor*, Washington.
- Montgomery, H.A.C., Dymock, J.F., 1961. The determination of nitrite in water. *Analyst* 86, 414–416.
- Nerenberg, R., 2016. The membrane-biofilm reactor (MBfR) as a counter-diffusional biofilm process. *Curr. Opin. Biotechnol.* 38, 131–136.
- Oksanen, J., Blanchet, G., Friendly, M., Kindt, R., Legendre, P., McGlenn, D., Minchin, P.R., O'Hara, R.B., Simpson, G.L., Solymos, P., Stevens, H., Szoecs, E. and Wagner, H. (2016) *vegan: Community Ecology Package*. R package version 2.4-0. <https://CRAN.R-project.org/package=vegan>.
- Oosterhuis, M., van Loosdrecht, M.C.M., 2009. Nitrification of urine for H<sub>2</sub>S control in pressure sewers. *Water Pract. Technol.* 4 (3).
- Pellicer-Nächer, C., Sun, S., Lackner, S., Terada, A., Schreiber, F., Zhou, Q., Smets, B.F., 2010. Sequential aeration of membrane-aerated biofilm reactors for high-rate autotrophic nitrogen removal: experimental demonstration. *Environ. Sci. Technol.* 44 (19), 7628–7634.
- De Paepe, J., De Pryck, L., Verliefe, A.R.D., Rabaey, K., Clauwaert, P., 2020. Electrochemically induced precipitation enables fresh urine stabilization and facilitates source separation. *Environ. Sci. Technol.*
- De Paepe, J., Lindeboom, R.E.F., Vanoppen, M., De Paepe, K., Demey, D., Coessens, W., Lamaze, B., Verliefe, A.R.D., Clauwaert, P., Vlaeminck, S.E., 2018. Refinery and concentration of nutrients from urine with electro dialysis enabled by upstream precipitation and nitrification. *Water Res.* 144, 76–86.
- De Paepe, K., Kerckhof, F.-M., Verspreet, J., Courtin, C.M., Van de Wiele, T., 2017. Inter-individual differences determine the outcome of wheat bran colonization by the human gut microbiome. *Environ. Microbiol.* 19 (8), 3251–3267.
- Quast, C., Pruesse, E., Yilmaz, P., Gerken, J., Schweer, T., Yarza, P., Peplies, J., Glockner, F.O., 2013. The SILVA ribosomal RNA gene database project: improved data processing and web-based tools. *Nucleic Acids Res.* 41 (D1), D590–D596.
- R Core Team, 2016. *R: A language and Environment for Statistical Computing*. R Foundation for Statistical Computing, Vienna, Austria <https://www.R-project.org/>.
- Rabaey, K., Boon, N., Siciliano, S.D., Verhaege, M., Verstraete, W., 2004. Biofuel cells select for microbial consortia that self-mediate electron transfer. *Appl. Environ. Microbiol.* 70 (9), 5373–5382.
- Ramette, A., 2007. Multivariate analyses in microbial ecology. *FEMS Microbiol. Ecol.* 62 (2), 142–160.
- Randall, D.G., Naidoo, V., 2018. Urine: the liquid gold of wastewater. *J. Environ. Chem. Eng.* 6 (2), 2627–2635.
- Salar-García, M.J., Ortiz-Martínez, V.M., Gajda, I., Greenman, J., Hernández-Fernández, F.J., Ieropoulos, I.A., 2017. Electricity production from human urine in ceramic microbial fuel cells with alternative non-fluorinated polymer binders for cathode construction. *Sep. Purif. Technol.* 187, 436–442.
- Schloss, P.D., Westcott, S.L., 2011. Assessing and improving methods used in operational taxonomic unit-based approaches for 16S rRNA gene sequence analysis. *Appl. Environ. Microbiol.* 77 (10), 3219–3226.
- Schloss, P.D., Westcott, S.L., Ryabin, T., Hall, J.R., Hartmann, M., Hollister, E.B., Lesniewski, R.A., Oakley, B.B., Parks, D.H., Robinson, C.J., Sahl, J.W., Stres, B., Thallinger, G.G., Van Horn, D.J., Weber, C.F., 2009. Introducing mothur: open-source, platform-independent, community-supported software for describing and comparing microbial communities. *Appl. Environ. Microbiol.* 75 (23), 7537–7541.
- Sprott, G.D., Patel, G.B., 1986. Ammonia toxicity in pure cultures of methanogenic bacteria. *Syst. Appl. Microbiol.* 7 (2), 358–363.
- Sun, F.Y., Dong, W.Y., Shao, M.F., Li, J., Peng, L.Y., 2012. Stabilization of source-separated urine by biological nitrification process: treatment performance and nitrate accumulation. *Water Sci. Technol.* 66 (7), 1491–1497.
- Tice, R.C., Kim, Y., 2014. Energy efficient reconcentration of diluted human urine using ion exchange membranes in bioelectrochemical systems. *Water Res.* 64, 61–72.
- Udert, K.M., Fux, C., Munster, M., Larsen, T.A., Siegrist, H., Gujer, W., 2003a. Nitrification and autotrophic denitrification of source-separated urine. *Water Sci. Technol.* 48 (1), 119–130.
- Udert, K.M., Larsen, T.A., Biebow, M., Gujer, W., 2003b. Urea hydrolysis and precipitation dynamics in a urine-collecting system. *Water Res.* 37 (11), 2571–2582.
- Udert, K.M., Larsen, T.A., Gujer, W., 2006. Fate of major compounds in source-separated urine. *Water Sci. Technol.* 54 (11–12), 413–420.
- Udert, K.M., Wächter, M., 2012. Complete nutrient recovery from source-separated urine by nitrification and distillation. *Water Res.* 46 (2), 453–464.
- Walter, X.A., Merino-Jiménez, I., Greenman, J., Ieropoulos, I., 2018. PEE POWER® urinal II – urinal scale-up with microbial fuel cell scale-down for improved lighting. *J. Power Sources* 392, 150–158.
- Wang, Q., Garrity, G.M., Tiedje, J.M., Cole, J.R., 2007. Naive Bayesian classifier for rapid assignment of rRNA sequences into the new bacterial taxonomy. *Appl. Environ. Microbiol.* 73 (16), 5261–5267.
- Wang, X.Y., Cai, Y.P., Sun, Y.J., Knight, R., Mai, V., 2012. Secondary structure information does not improve OTU assignment for partial 16S rRNA sequences. *ISME J.* 6 (7), 1277–1280.
- Wickham, H. (2009) *ggplot2: Elegant Graphics for Data Analysis*.
- Wilsenach, J., van Loosdrecht, M., 2003. Impact of separate urine collection on wastewater treatment systems. *Water Sci. Technol.* 48 (1), 103–110.
- Wohlsager, S., Clemens, J., Nguyet, P.T., Rechenburg, A., Arnold, U., 2010. Urine—a valuable fertilizer with low risk after storage in the tropics. *Water Environ. Res.* 82 (9), 840–847.
- Xing, D., Cheng, S., Logan, B.E., Regan, J.M., 2010. Isolation of the exoelectrogenic denitrifying bacterium *Comamonas denitrificans* based on dilution to extinction. *Appl. Microbiol. Biotechnol.* 85 (5), 1575–1587.
- Yenigün, O., Demirel, B., 2013. Ammonia inhibition in anaerobic digestion: a review. *Process Biochem.* 48 (5), 901–911.